MEDICAL NOW Digest

No.88 2021

SHIMADZU

CONTENTS

RAD

Experience with RADspeed Pro style edition and Dynamic Chest Radiography

Taku Kuramoto, R.T.

Division of Radiology, Department of Medical Technology, Kyushu University Hospital[1]
Department of Clinical Radiology, Graduate School of Medical Sciences, Kyushu University[2]
Taku Kuramoto[1], Hideki Yoshikawa[1], Akiko Hattori[1], Yuzo Yamasaki[2], Tomoyuki Hida[2], Takeshi Kamitani[2], Toyoyuki Kato[1], Kousei Ishigami[2]

1. Hospital Introduction

Kyushu University Hospital **(Fig. 1)** is located in Higashi-ku, Fukuoka City, Fukuoka Prefecture, and its branch hospital, Kyushu University Beppu Hospital, is located in Beppu City, Oita Prefecture. Kyushu University Hospital has 1,275 beds and is one of the largest national university hospitals in Japan with 752,416 outpatients (3,083.7 per day) and 413,987 inpatients (1,134.2 per day) in 2018. Kyushu University Hospital is also a “core hospital” responsible for advanced medical care in the western region of Japan and tasked with safely providing the latest and best medical care.
The Division of Radiology at Kyushu University Hospital operates with 5 physicians (2 with shared appointments), 67 radiological technologists, 10 nurses, and 10 clerical assistants. The division also works with more than 30 radiologists.

Fig.1 Exterior of Kyushu University Hospital (main site)

2. Equipment Characteristics

The RADspeed Pro style edition digital radiography system was first launched commercially in November 2018. When combined with Konica Minolta’s AeroDR fine digital radiography system, RADspeed Pro style edition is also capable of performing dynamic chest radiography. In March 2019, a RADspeed Pro style edition system was installed in 1 of our hospital’s 9 general (plain) radiography rooms (3 rooms for chest and abdominal radiography, 5 rooms for skeletal radiography, and 1 room for pediatric radiography). Because RADspeed Pro style edition is designed not just for dynamic chest radiography but also for use as a general radiography system, it provides good ease-of-use for applications other than dynamic chest radiography and a high level of versatility to perform various examinations. RADspeed Pro style edition also comes with a variety of functions and applications, some described below, and is designed to accommodate the wide-ranging needs of medical institutions **(Fig. 2)**.

(1) Auto-positioning function:
A single touch of the included remote control automatically maneuvers the ceiling-mounted X-ray tube support to a set position.
(2) Flat panel detector (FPD) auto-tracking function:
The longitudinal position of the FPD inside the Bucky table (supine radiography) is automatically linked to the position and angle of the X-ray tube unit.
(3) Vertical tracking function:
The focal height of the X-ray tube unit is linked to the Bucky stand and Bucky table height.
(4) Long view radiography function:
During radiography, the irradiation angle of the X-ray tube unit moves automatically to match the movement of the FPD when acquiring images. The acquired images are also automatically stitched together by the DR system.
(5) REALISM processing: A new image processing engine
(6) Intelligent Grid: An image processing technology for scatter correction
(7) Bone suppression: Thoracic bone attenuation processing

etc.

※ (5) to (7) are functions performed by the Konica Minolta DR system.

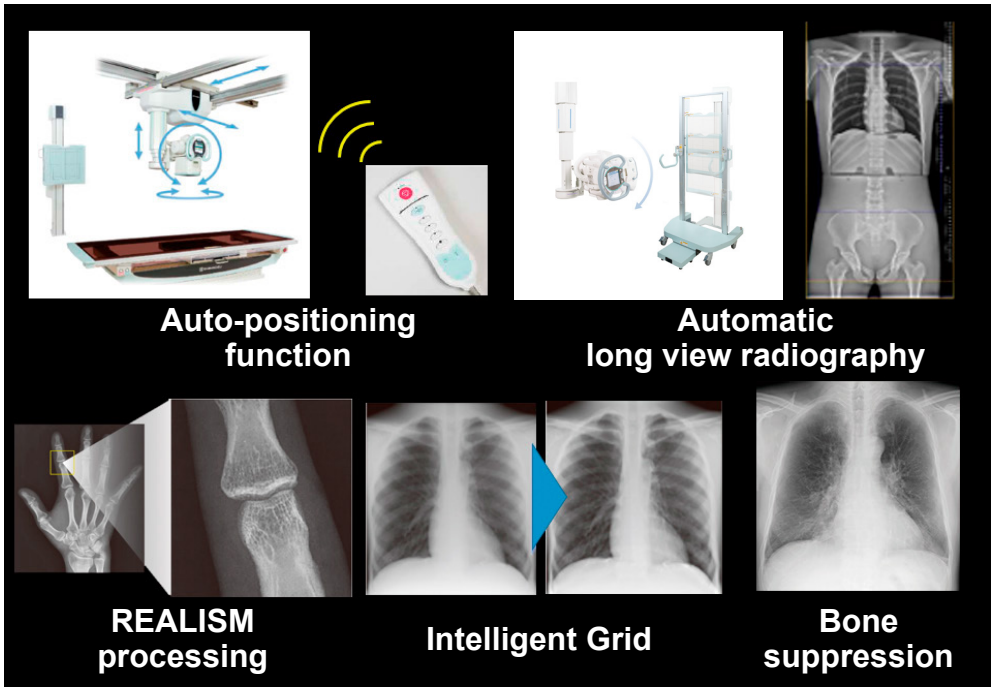

Fig.2 Various Functions and Applications for RADspeed Pro style edition

The FPD inside the Bucky stand and Bucky table can also be removed and used wirelessly to accommodate radiography of the head and extremities.

3. Image Transfer

The DR system can acquire two types of images: general radiographs (static images) and dynamic radiographic images (dynamic images). The image transfer workflow is shown in Fig. 3. After acquisition, static images are sent from the console to an image checking terminal, then transferred to the picture archiving and communication system (PACS). By contrast, dynamic images are transferred to a dynamic image analysis workstation to undergo sequential analysis processing, and the results of this processing are then transferred to the PACS. Static images and dynamic images can both be viewed from any terminal in the hospital.

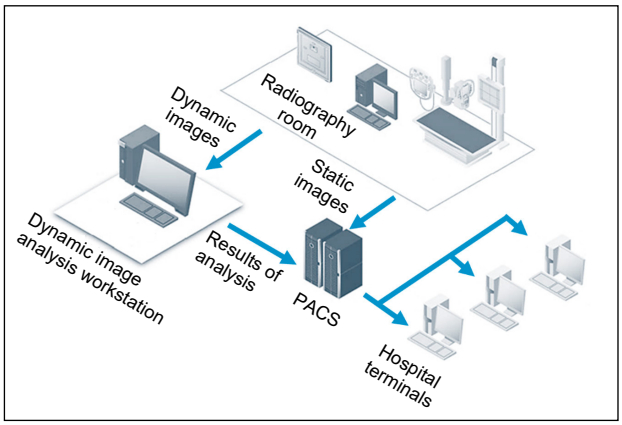

Fig.3 Image Transfer Workflow

4. Dynamic Radiography at Kyushu University Hospital

Kyushu University Hospital performs two types of dynamic radiography, a “deep breathing protocol” that acquires images during approx. 1.5 deep breaths and a “breath-holding protocol” that acquires images in a state of maximal inspiration where both protocols are performed upright or supine. The purpose of the deep breathing protocol is, through applying dynamic image analysis, to visualize signal changes associated with respiration, and the purpose of the breath-holding protocol is to visualize signal changes that occur in synchronization with the heartbeat. Each protocol is shown in detail in Fig. 4. The deep breathing protocol and breath-holding protocol require different guidance on breathing, hence different explanations and voiced instructions are provided to patients for each protocol.

5. Notes on Radiography

Images acquired by dynamic chest radiography are transferred to a dynamic image analysis workstation where, between each consecutively acquired image,

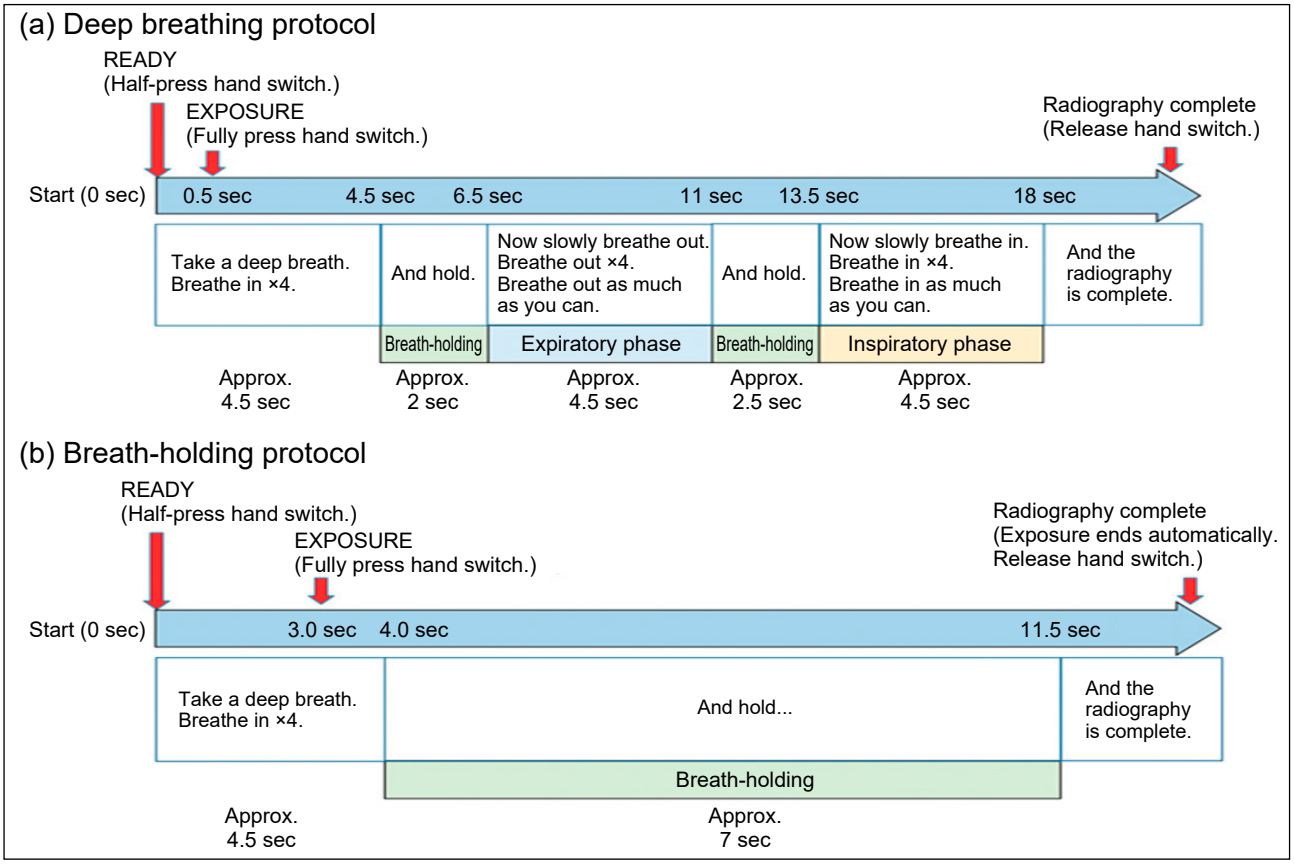

Fig.4 Two Dynamic Radiography Protocols Used by Kyushu University Hospital

pixel value changes arising from the physiological activity of tissue within the pulmonary field, such as alveoli and pulmonary arteries, are enhanced and undergo color-mapping analysis. During acquisition, patient movement other than respiratory movement or cardiac movement must be avoided because it can cause unwanted pixel value changes. Only pixel value changes caused by the movement of specific tissues within the pulmonary field are needed for dynamic analysis. For standing radiography of the chest performed in the posterior-anterior direction, image processing is prone to fail when an angle of 5 or more degrees is present between the patient and FPD laterally or anteroposteriorly. For this reason, the patient is immobilized as much as possible during acquisition to minimize body movement and maintain a correct body posture (Fig. 5). Specifically, the patient stands with feet at shoulder width and is attached to a Bucky stand by a belt around the pelvis. The patient also grasps front handles on the stand and positions their jaw slightly touching but not resting on a chin rest. During the deep breathing protocol, respiration may also cause patients to move their shoulders vertically, hence breathing exercises are performed beforehand so patients fully understand the type of imaging being performed and what precautions must be taken.

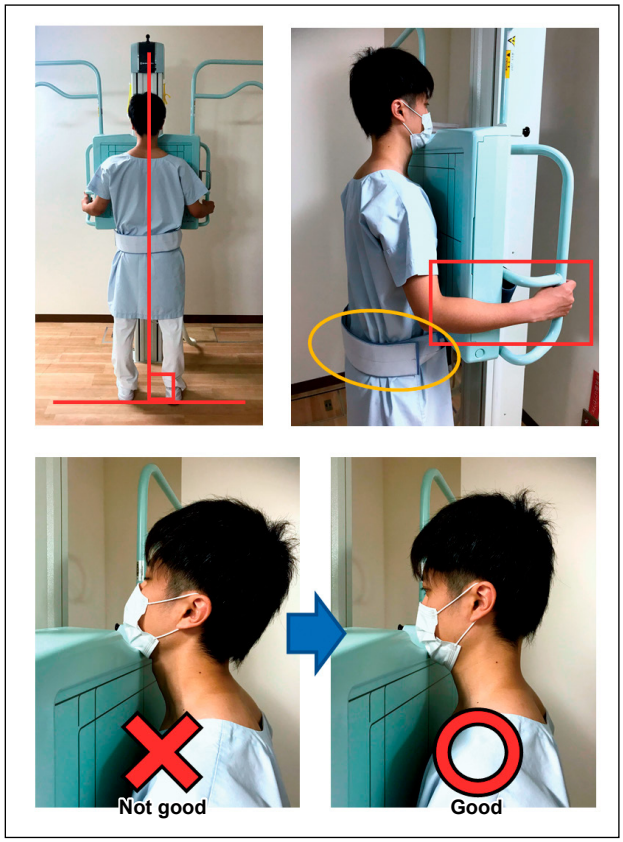

Fig.5 Positioning Measures for Standing Radiography

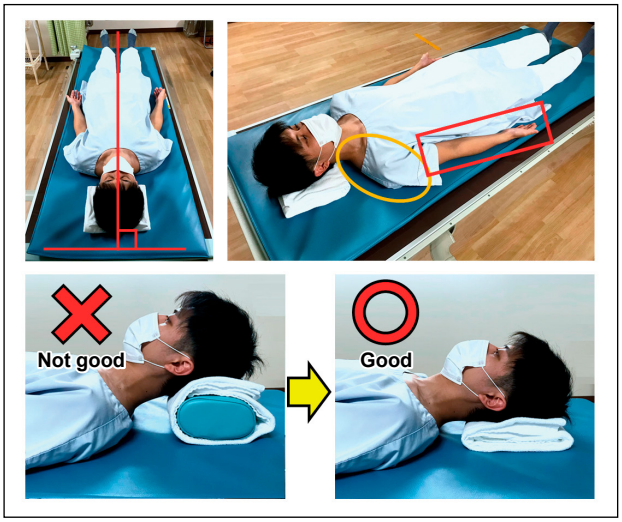

Fig.6 Positioning Measures for Supine Radiography

For supine radiography performed in the anterior-posterior direction, patients are placed in a fully relaxed position that includes the shoulders with elbows extended and palms facing upward. The pillow used for normal radiography raises the head, flexes the neck, and lowers the chin an excessive amount, hence a folded bath towel is used instead of a pillow (Fig. 6). Based on the range of motion of the equipment and the magnification of the subject, the source-to-image distance (SID) is set to 200 cm for standing radiography and 150 cm for supine radiography.

6. Exposure Conditions

No detailed investigations had been performed or reports published on optimizing exposure conditions for dynamic chest radiography. We investigated approaches to setting exposure conditions based on the body type of the patient. Basing this investigation on exposure conditions and patient body thickness and body type, patients were divided into three groups based on body mass index (BMI) and each examined with a different radiography tube voltage: (1) 85 kV for BMI < 17, (2) 100 kV for 17 ≤ BMI ≤ 25, and (3) 110 kV for 25 < BMI. Using the exposure conditions shown in (1), (2), and (3) above, the relationship between subject BMI and an image sensitivity indicator (S-value) measured clinically is shown in Fig. 7. When a value within 3,000 is taken as the target S-value for dynamic chest radiography images, at least 90 % of all images fell within this target. We now plan an extended study that focuses on S-values close to the target value and optimizes for these cases.

Based on the literature, the X-ray dose for dynamic chest radiography is approx. 1.5 mGy[1], which is lower than the guidance level for plain chest radiography (frontal chest view: 0.4 mGy, lateral chest view: 1.5 mGy, total: 1.9 mGy)[2] recommended by the International Atomic Energy Agency (IAEA). After the RADspeed Pro style edition was introduced to our hospital, entrance surface dose (ESD) measurements were taken to validate the exposure conditions used by our hospital. Exposure conditions were set to dynamic chest radiography conditionsused on a patient of standard body type (100 kV, 80 mA, 8 ms, Cu filter: 0.2 mm) with the breath-holding protocol. For comparison, ESD measurements were also taken in frontal view and lateral view with exposure conditions used for plain chest radiography. The results are shown in Fig. 8. The ESD for dynamic chest radiography was 1.24 mGy, higher than plain chest radiography but also lower than the IAEA guidance level (total of frontal

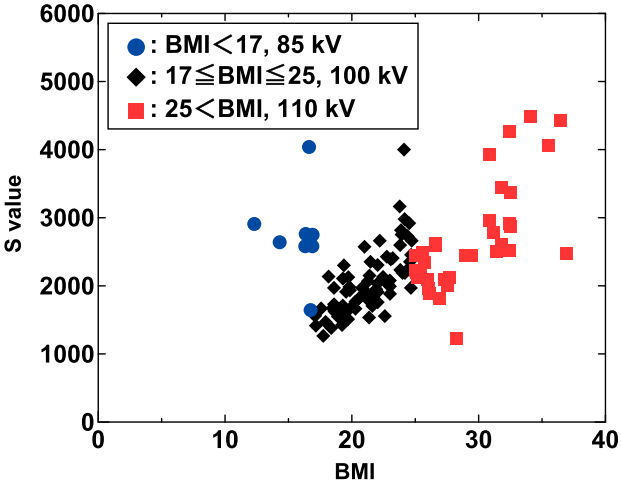

Fig.7 Relationship between BMI of Patients and S-Value of Acquired Images

Dose Comparison

	kV	mA	ms	Time (s)	Cu (mm)	Dose (mGy)
Dynamic breath-holding	**100**	**80**	**8**	**7**	**0.2**	**1.24**
Frontal chest	120	160	20	-	0.1	0.12
Lateral chest	140	125	63	-	0.1	0.40
					Total	**0.52**

IAEA Guidance Level	Dose (mGy)	Medical Exposure Guidelines by Japan Association of Radiological Technologists	Dose (mGy)
Frontal chest	0.4	Frontal chest*	0.3
Lateral chest	1.5	Lateral chest**	0.8
Total	1.9	Total	1.1

*DRLs2015 ** Medical exposure guidelines 2006

Fig.8 Comparison of Measured Data and Guideline Values

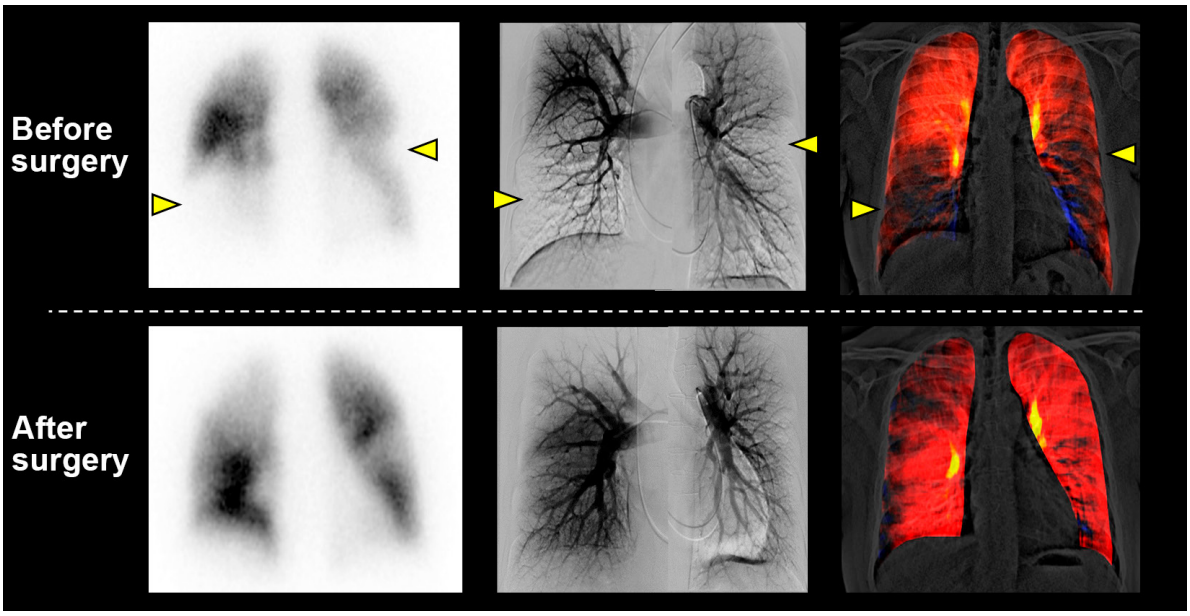

Fig.9 Images of CTEPH Patient Acquired by Different Examination Methods

and lateral views). For reference, we also compared this result obtained using the breath-holding protocol to guidelines established in Japan. The 1.24 mGy ESD measured for dynamic chest radiography was slightly higher than the 1.1 mGy ESD total for frontal and lateral chest views that appears in Japanese guidelines.

We have only just started seeing clinical applications of dynamic chest radiography, hence further study is needed to quickly establish standard exposure conditions for this imaging method. Further study is also needed into the validity of a simple X-ray dose comparison with plain chest radiography.

7. Work at Kyushu University Hospital

More than 180 image acquisitions have been performed by RADspeed Pro style edition and dynamic chest radiography system since its introduction (as of September 4, 2020). Described below are two cases in which the system demonstrated its usefulness.

Fig. 9 shows Tc-99m MAA lung perfusion scintigraphy images (left), pulmonary angiography images (middle), and dynamic chest radiography images (right) from a patient diagnosed with chronic thromboembolic pulmonary hypertension (CTEPH)[3]. The preoperative Tc-99m MAA lung perfusion scintigraphy image shows multiple perfusion defects in both lung fields, which are also visible in the pulmonary angiography image (▻). A pulmonary circulation image generated from the dynamic chest radiography also shows similar findings. The bottom row in Fig. 9 shows images acquired by respective examinations after the patient underwent pulmonary endarterectomy (PEA). After PEA, the pulmonary hypertension was improved and all examination results revealed improved pulmonary blood flow in both lower lung fields. This shows that images of pulmonary circulation image obtained by dynamic chest radiography can potentially be used to assess pulmonary circulation in patients with CTEPH.

Next, Fig. 10 shows lung ventilation and perfusion scintigraphy images (top left: ventilation, top right: perfusion) and dynamic chest radiography images (bottom left: ventilation, bottom right: pulmonary circulation) from a patient examined for shortness

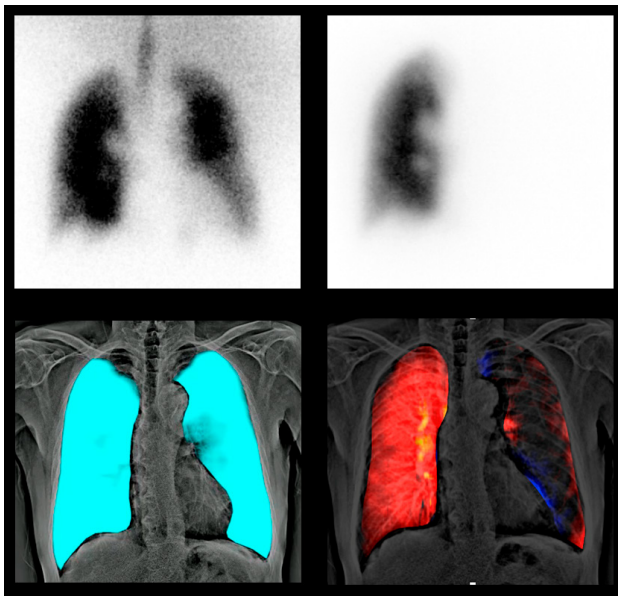

Fig.10 Images of Patient Diagnosed with Blockage of the Left Pulmonary Artery

of breath on exertion[4]. Dynamic chest radiography images reveal a pulmonary ventilation-perfusion mismatch in the left lung and the lung ventilation-perfusion scintigraphy images show similar findings. Based on further examinations, the patient was diagnosed with blockage of the left pulmonary artery caused by vasculitis. These findings show that dynamic chest radiography can potentially visualize even small pixel value changes caused by filling of the lungs with air during respiration (ventilation image) and blood supply during breath-holding (pulmonary circulation image) , without the need for contrast media or radioisotopes (radionuclides).

8. Conclusion

This article describes our experience using a RADspeed Pro style edition digital radiography system and dynamic chest radiography system newly installed at Kyushu University Hospital. Compared to angiographic examinations and nuclear scanning, dynamic chest radiography is a simpler imaging method but can potentially achieve equivalent diagnostic results. Although further clinical studies are needed to demonstrate the utility of dynamic chest radiography, it promises to be a useful alternative diagnostic tool for clinics unable to perform angiographic examinations or nuclear scanning and for medical sites in developing countries.

References

1) Matsutani N. Visualization and Quantitation of Physiological Function by Dynamic Analysis—the Next Stage in Plain Radiography— JIRA Technical Report, 29 (2), 2019
2) IAEA, 1996. International Basic Safety Standard for Protection against Ionizing Radiation and for the Safety of Radiation Source.Safety Series No.115.
3) Yamasaki Y et al. A novel pulmonary circulation imaging using dynamic digital radiography for chronic thromboembolic pulmonary hypertension. European Heart Journal, 41 (26), 2020
4) Yamasaki Y et al. Pulmonary ventilation–perfusion mismatch demonstrated by dynamic chest radiography in giant cell arteritis. European Heart Journal, 2020.

RAD

GLIDE Technologies™ Smooth Action that Mirrors Operator Intent

Global Marketing Department, Medical Systems Division, Shimadzu Corporation[1]
Research & Development Department, Medical Systems Division, Shimadzu Corporation[2]
Tomoharu Okuno[1], Ken Shirota[2]

1. Introduction

In medical settings, X-ray diagnostic imaging systems are designed with support systems that provide a stable platform for heavy components such as the X-ray tube and collimator that use lead to prevent radiation leakage and provide a convenient means of moving the imaging system into the desired radiography position. These support systems must be sufficiently strong and durable to perform these tasks and have well-balanced weight that allows easy manipulation. These support systems can make X-ray diagnostic imaging systems weigh as much as several hundred kilograms. Although it is important that X-ray systems are positioned for each individual examination and patient, performing this manually would entail repeatedly moving a very heavy mass and place a tremendous burden on the operator that risks shoulder discomfort and back pain. If positioning is not performed smoothly and trouble-free, it also places a greater burden on the patient by lengthening the time required to hold a instructed posture.

To improve the examination environment with respect to these issues, Shimadzu equips its general radiography systems, mobile X-ray systems, and fluoroscopy systems with proprietary GLIDE Technologies. GLIDE Technologies ensure smooth action that mirrors operator intent even for medical systems weighing several hundred kilograms. This article describes these GLIDE Technologies.

2. The Elemental Technologies of GLIDE Technologies

The “GLIDE” name ascribed to GLIDE Technologies refers to gliding-like movement. GLIDE Technologies used five elemental technologies to achieve this gliding-like movement: sensing technology, torque control technology, shock reduction technology, stability control technology, and balance technology. The development of these technologies was driven by engineers’ passion to improve the examination environment and improve the operability of medical systems.

• Sensing Technology

One of the methods by which effortless movement is achieved is through power assistance. The challenge faced by power assist technology is, while power assist functions move the system in the direction of force applied by the operator at a given moment, the force applied by the operator is constantly changing. Sensing technology plays a vital role in accurate force detection when both the operator and medical system are in motion, and this technical expertise is integrated into control handles that have undergone repeated prototyping (Fig. 1).

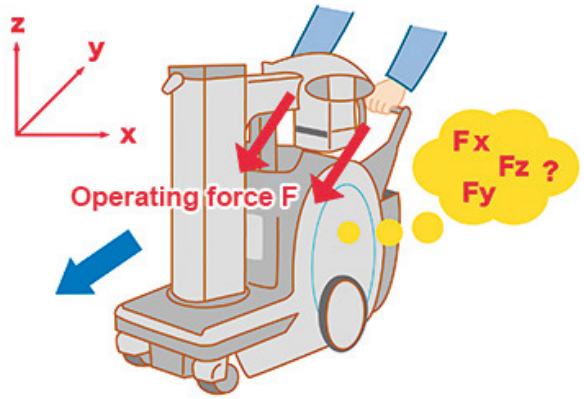

Fig.1 Sensing Technology

• Torque Control Technology

F = Ma. Effecting the operator’s intended action may appear a simple question of adjusting the speed and acceleration of the medical system based on this common physical law, but, in practice, a control scheme based purely on speed and acceleration could not eliminate “unnaturalness” from medical system movement. The root cause of this

"unnaturalness" was feedback delay and cumulative error. To resolve this problem, motor and system characteristics were revised and a compensating torque control was devised that consistently transmits accurate torque levels with no delay. This approach successfully eliminated "unnaturalness" from medical system movement (Fig. 2).

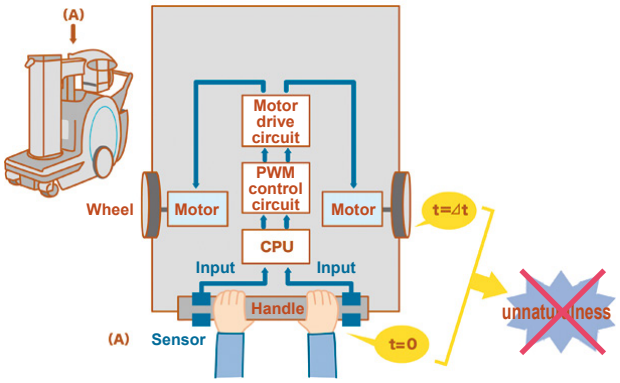

Fig.2 Torque Control Technology

• Shock Reduction Technology

Power assist technology must be able to control medical systems so that the response of the medical system aligns with the operator's sensations. For example, when an operator attempts to move a medical system from a standstill, the operator applies a greater force on the control handle than they expect. When this force is transmitted unmodified, the unit suddenly jerks forward with a shuddering motion. Experimentation revealed that, for the same amount of force detected by the sensor, the force applied in the operator's estimation differed depending on the drive state of the system and the movement of the operator. A long period of trial and error was required to eliminate this shudder, or "unnaturalness," which was eventually eliminated using speed-dependent torque control technology (shock reduction technology) (Fig. 3).

• Stability Control Technology

In order to accommodate the variable force applied by the operator and move the medical system in line with operator intent, force must be detected in multiple directions and the medical system moved in the appropriate direction. However, straight-line stability and directional responsiveness tend to work in opposition to one another. Stability control technology was developed that adjusts the balance between straight-line stability and directional responsiveness based on system installation and usage scenario (Fig. 4).

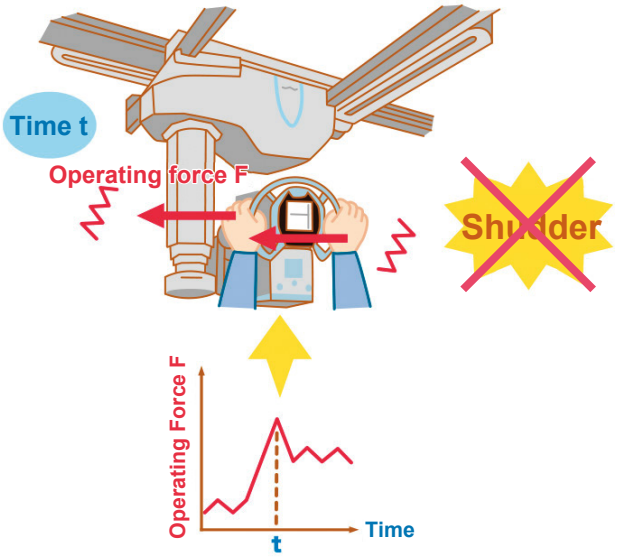

Fig.3 Shock Reduction Technology

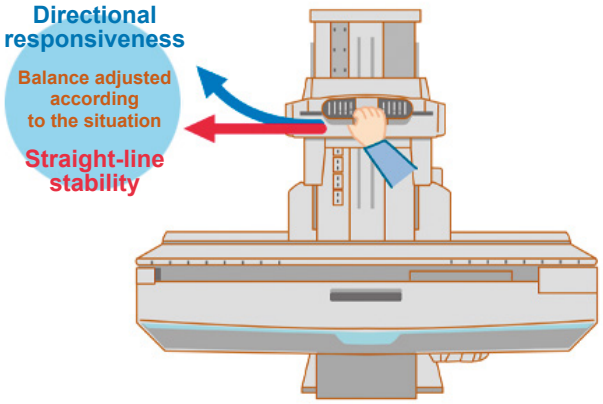

Fig.4 Stability Control Technology

• Balance Technology

Major components, such as the X-ray tube, are attached to the support column on medical systems. Shimadzu's mobile X-ray systems use a collapsible support column to prevent the support column from impeding the operator's forward view during travel and to provide good visibility. A key part of the collapsible support column is a spring and wire that form a spring-balanced mechanism. This mechanism is designed to transmit power to the spring as the wire winds around a spiral-shaped pulley. This absorbs the change in elastic force generated in the spring during column extension and creates a smooth collapsible movement over the column's entire range of extension (Fig. 5).

3. Shimadzu Products Featuring "GLIDE Technologies"

Shimadzu's MobileDaRt Evolution™ MX8 Version mobile X-ray system is equipped with GLIDE

VIEW™ function, a GLIDE Technology that allows for smooth support column extension and efficient and safe travel. Shimadzu's FLUOROspeed™ X1 edition patient-side R/F system (for the US market) is designed for a mode of operation mainly in demand in the USA where physicians or radiological technologists operate the equipment at the table-side (fluoroscopy table) while medical care is provided to the subject. FLUOROspeed™ X1 edition system is equipped with a GLIDE ASSIST™ function that allows for smooth manipulation of the imaging deck.
A new part of Shimadzu's product lineup is the RADspeed™ Pro style edition general radiography system, which is equipped with a POWER GLIDE™ function that allows for smooth positioning of the X-ray tube **(Fig. 6)**.

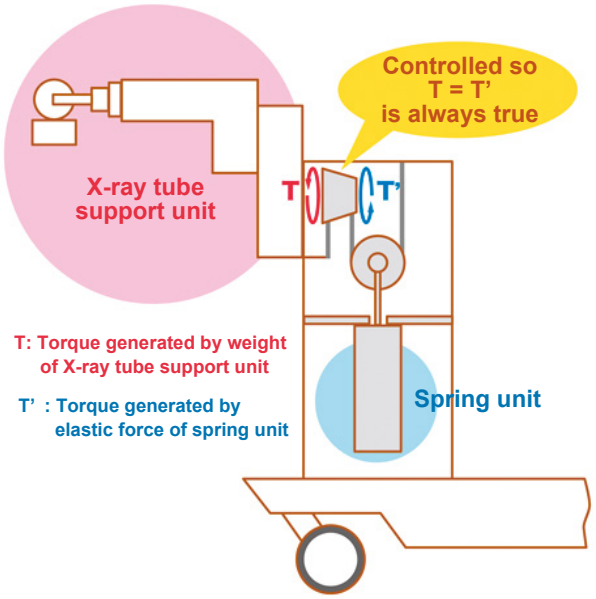

Fig.5 Balance Technology

4. GLIDE Technologies in General Radiography Systems

General radiography systems are used during basic examinations in diagnostic imaging and carry out many examinations daily and acquire images of a variety of sites from the head to the chest, abdomen, arms and legs. To improve workflows in busy medical sites, Shimadzu's RADspeed Pro style edition general radiography system **(Fig. 7)** has supported radiography parameters synchronizing, X-ray irradiation synchronizing, auto-positioning, and various other functions.
Despite these functions, the final deciding step in radiography is manual positioning of the X-ray tube. The operator of a general radiography system may need to alter the position of an X-ray tube located as far as 180 cm from the patient and carefully position the X-ray tube to ensure an irradiation field within several millimeters of the desired field of view. The POWER GLIDE power assist function was developed to improve the examination environment by meeting the high demands for system operability in clinical settings while reducing the burden on the operator and patient, thereby providing additional improvements in workflow.

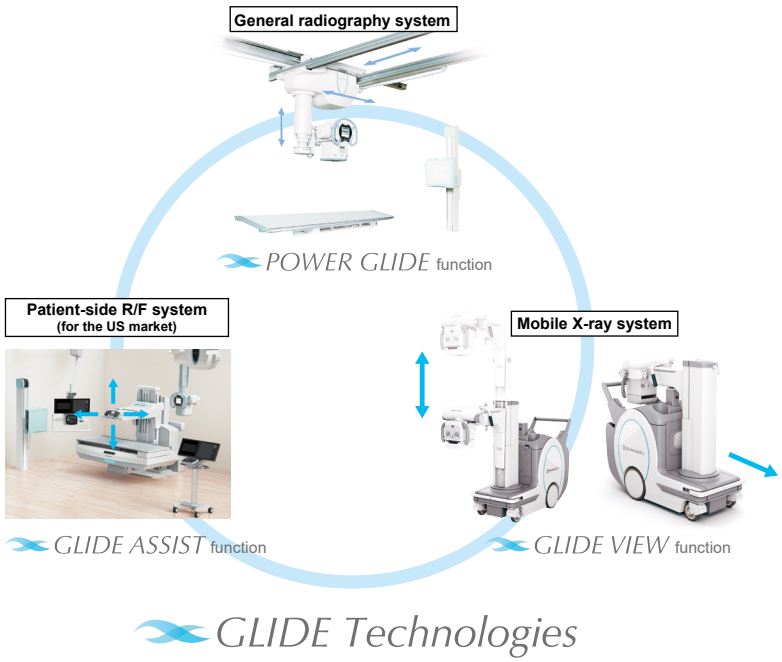

Fig.6 Shimadzu Products Featuring "GLIDE Technologies"

Fig.7 RADspeed Pro style edition General Radiography System

(1) Smooth Operation Even with One-Handed Control

Shimadzu expanded the use of its well-regarded power assist technology, normally found in Shimadzu's MobileDaRt Evolution MX8 Version mobile X-ray system, and integrated it into the RADspeed Pro general radiography system for smooth operation even with one-handed control of systems weighing as much as 300 kg. Without POWER GLIDE, over 3 kg of force was needed to start moving the unit from a standstill, but with POWER GLIDE, just 1 kg of force or less is needed to start moving the unit. It reduces the burden on the operator by two-thirds enabling a substantial reduction in manual labor.

Force sensors can also detect very small forces on the X-ray tube support handle and allow constant control of system motors via optimum output signals in three axes (longitudinal, transversal, and vertical axes). The angle of handle rotation is also transformed into coordinates in real-time, providing system operability with no awkwardness even during rotation-controlled movement.

(2) Adjustable Power Assist Level Based on Usage

Along with excellent operability, three power assist levels can be selected via the touch-screen control panel on the X-ray tube support **(Fig. 8)**. The power assist level is adjustable to accommodate various scenarios, such as reducing the assist level for radiography that requires fine positioning, and increasing the assist level when rapid system movement is required, such as moving between standing and supine radiography. Turning the collimator lamp on also automatically reduces the assist level, assisting with fine positioning.

Furthermore, the acceleration (Acc), deceleration (Dec), and maximum speed (Speed) of each assist level can be adjusted at any time **(Fig. 9)**. During configuration at installation, password protection can also be applied so only a manager can change the settings.

Fig.8 Assist Level Switching Screen

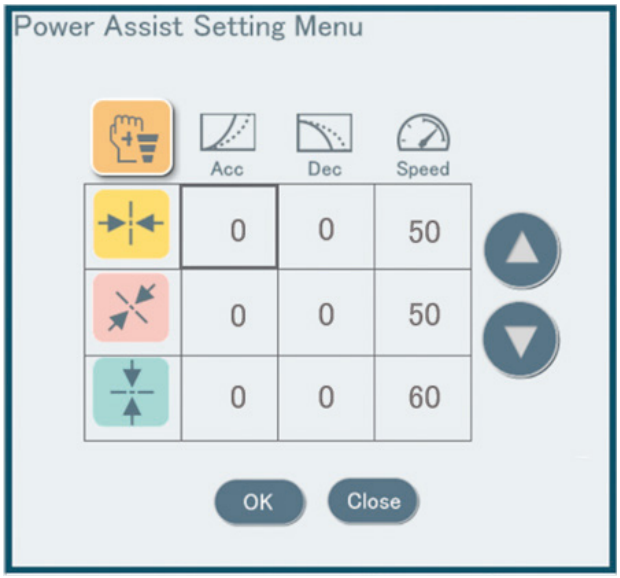

Fig.9 Assist Level Configuration Screen

(3) Improved Operation of Rear Button Array

A vertical axis rotation button, "all-free" button, and collimator lamp button are found on the column of the X-ray tube support on the past Shimadzu systems **(Fig. 10a)**. When the front control panel is not accessible during positioning, these operations can be performed via a rear button array found on the rear of the system. The placement of this button array has been evaluated that it has detailed

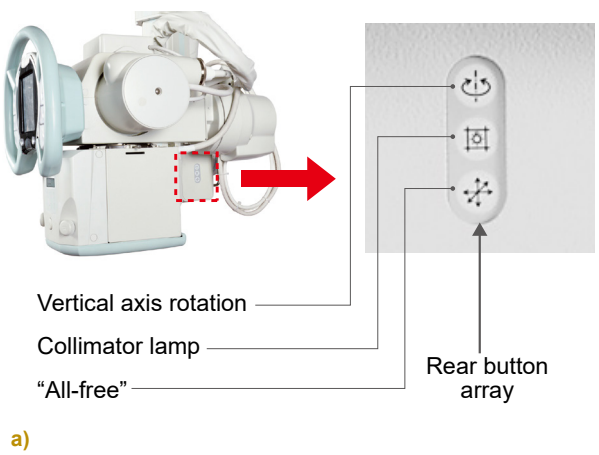

a)

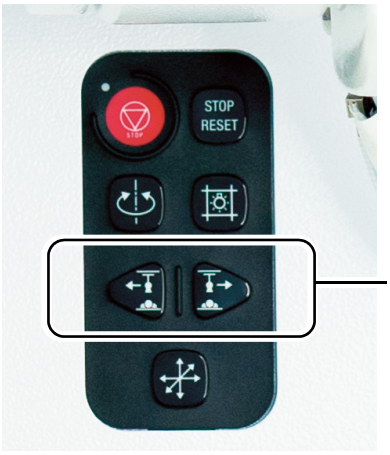

b)

Fig.10 Rear Button Array on X-Ray Tube Support
a) Without POWER GLIDE
b) With POWER GLIDE

consideration from the viewpoint of the medical site. When POWER GLIDE is added, a new single-axis movement buttons are also included **(Fig. 10b)**. Pressing these buttons move the system at a constant velocity in a pre-configured direction. When multiple operators are engaged in positioning, this allows the X-ray tube support to be operated stress-free from the rear and delivered to another operator in front of the system, or the X-ray tube support can be operated stress-free from the rear while the patient alights from the Bucky table.

5. Summary

This article described GLIDE Technologies that aim to improve the examination environment in medical sites by enabling smooth, stress-free system movement that mirrors operator intent.

POWER GLIDE is a newly introduced GLIDE Technology that ensures smoother and more effortless positioning of X-ray tubes on general radiography systems. POWER GLIDE reduces the physical burden on the shoulder and back of operators, reducing the risk of shoulder discomfort and back pain. POWER GLIDE promises to substantially reduce the burden on the operator and improve the examination environment. By providing additional improvements in workflow, it also shortens the duration of time patients must maintain a instructed posture and helps with efficient examinations.
Shimadzu will continue to refine GLIDE Technologies and various other technologies to improve the quality of medical care.

Minimally Invasive Procedures in Practice

Medical Systems Division, Shimadzu Corporation

Ayumi Iwata

As interventional procedures become increasingly complex and advanced, there is a demand for angiography systems that reduce X-ray doses, reduce contrast medium usage, and shorten examination times. Shimadzu's latest Trinias series angiography system features various functionality for achieving minimally invasive procedures.

This article compiles some of Shimadzu's initiatives in minimally invasive treatment that have received particularly high praise.

1 Initiatives to Reduce X-Ray Doses — Low Dose Fluoroscopy Mode and SCORE RSM —

The International Commission on Radiological Protection (ICRP) poses the general principle that X-ray doses should be reduced to As Low As Reasonably Achievable (ALARA), and as seen by the increasing number of countries to establish Diagnostic Reference Levels (DRLs), awareness of X-ray dose reduction has increased substantially. In light of this, the low dose fluoroscopy mode(preset name : Low) available in Trinias series systems has been particularly well-received. This low dose fluoroscopy mode can be used irrespective of region of treatment (excluding pediatrics) and reduces X-ray doses by 44 % or more compared to normal dose fluoroscopy mode **(Fig. 1)**. It is also provided with an ultra-low dose fluoroscopy mode (preset name:ExLow / Lowest) dedicated to catheter ablation treatment. Thanks to the motion tracking Noise Reduction technology, which is the core technology of our image processing engine named "SCORE PRO Advance", enables to minimize the afterimage even fluoroscopy at low pulse rate. Therefore, further dose reductions can be achieved by combining ultra-low dose fluoroscopy mode with low pulse rates in the arrhythmia therapy. All Trinias series models are equipped with these low dose modes as standard, and this "Minimally Invasive Treatment in Practice" section compiles various first-hand accounts from facilities that reduced doses with these low dose modes.

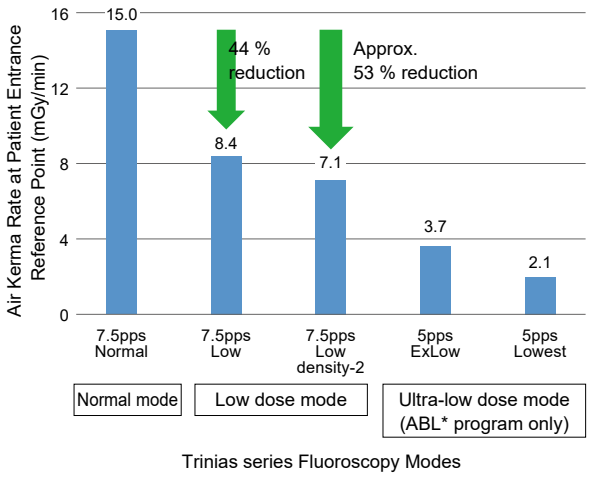

Fig. 1 Comparison of X-Ray Doses in each Fluoroscopy Mode
(Cardio/ ABL* fluoroscopy program)
(FOV 6 inch, acrylic 20 cm, SID 100 cm, calculated values for 7.5 pps Low density-2)
* Dedicated program for the catheter ablation treatment in the arrhythmia therapy

SCORE RSM is another Shimadzu's initiative to lower X-ray doses. SCORE RSM is a Shimadzu's proprietary imaging technique that generates a low frequency mask image from live images and performs frequency subtraction processing in real time. SCORE RSM is excellent at visualizing small contrast-enhanced vessels and devices and its dose per pulse is approx. 34 % lower than that of standard High-Speed (HS) DSA **(Fig. 2)**. The principal advantage of SCORE RSM is a high tolerance for subject movement due to frame-by-frame processing, and some medical facilities have utilized this feature to reduce total doses on each procedure by effectively selecting between using SCORE RSM or DSA imaging. Since SCORE RSM does not require breath holding and is not affected by misregistration due to intestinal

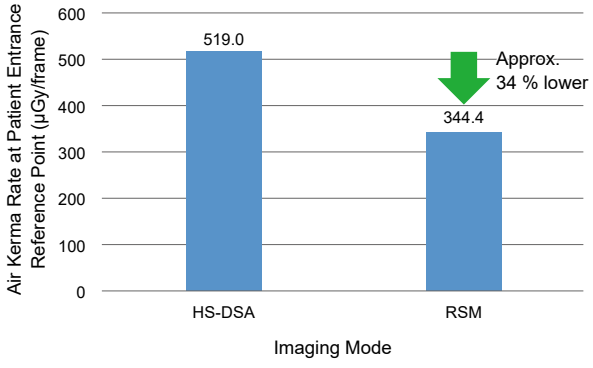

Fig. 2 X-Ray Dose Comparison between HS-DSA and SCORE RSM
(FOV 8 inch, acrylic 20 cm, SID 100 cm)

movements, there are many cases of switching from DSA imaging to SCORE RSM imaging. It is highly evaluated that this can be expected to further reduce the dose.

2 Initiatives to Reduce Contrast Medium Use — SCORE Chase —

Shimadzu has been also engaged in developing functions that reduce contrast medium use.

One of these initiatives is SCORE Chase, an application that generates long-view images of the lower extremities **(Fig. 3)**. SCORE Chase can generate long-view images and allow observation of the entire lower extremities from a single contrast injection image acquisition. Long-view images can be created both by panning catheter table lateral and longitudinal direction and SCORE Chase is also suitable for patients with joint mobility issues. By combining SCORE Chase with the ability of SCORE RSM to tolerate patient movement, unsuccessful acquisitions and repeated acquisitions can be avoided and ineffectual use of contrast media can be reduced. A long-view image is also generated automatically as soon as the acquisition is complete, allowing for easy overall comparison of blood flow features before and after treatment and hence shorter examination times.

Fig. 3 RSM Long-View Image with SCORE Chase

3 Initiatives to Shorten Examination Times — Shimadzu's Proprietary Procedure Support Functions —

SMART Access function of the C-arm positioner was developed for shorter examination times and has been well-received. Shimadzu's proprietary C-arm axle structure enables Transversal movement that accommodates a radial approach with a single-plane and frontal C-arm of bi-plane system. This SMART Access function has received high praise for enabling the trouble-free implementation of all steps from patient entry, to C-arm positioning, diagnosis, and treatment in sites where space is at a premium. SMART Touch is a customizable touch panel mountable at the bedside that can be used to change the fluoroscopy or radiography program, select applications, and perform image operations during procedure. SMART Touch is well evaluated as providing the stress-free operation because the required functions can be customized for each procedure and operator.

Another area of development is imaging that combines SCORE RSM with precessional C-arm movement. SCORE RSM precessional imaging allows images to be acquired from multiple directions in a single contrast injection image acquisition. Furthermore, by selecting a frame with well-separated blood vessels from the acquired images and transmitting the angle information of that frame to the C-arm, the optimum angle can be reproduced quickly. **(Fig. 4)**. This can even be performed at a single touch and has been highly praised for facilitating speedy progress during procedures.

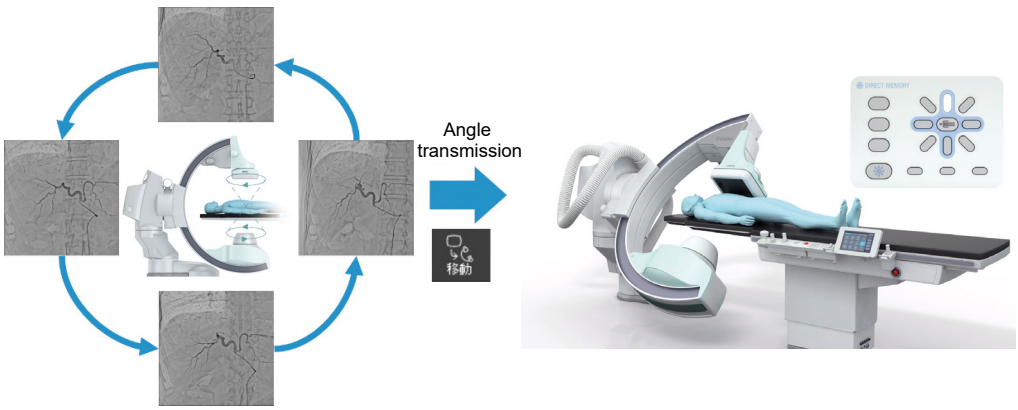

Fig. 4 Precessional Imaging and Angle Transmission

4 Final Comments

Shimadzu has ceaselessly pursued the development of image-guided applications for real-time performance and proprietary procedure-support functions aimed at minimally invasive treatments. Going forward, Shimadzu will continue to collect feedback from all parties engaged in interventional procedures and endeavor to make interventions even less invasive.

Dedicated Breast PET

Experience Using the Elmammo Dedicated Breast PET System

Shima Inoue, R.T.

Radiological Technology Department, Clinical Technology Division, MI Clinic
Shima Inoue

1. Clinic Overview

MI Clinic was opened in November 2005 in Toyonaka City, northern Osaka Prefecture. MI Clinic **(Fig. 1)** is a diagnostic imaging center that only accepts referred patients and is primarily focused on local health care. Located just three monorail stops from Osaka International (Itami) Airport, MI Clinic sees a significant number of foreigners and Japanese patients from other prefectures as well as Osaka residents.

The main diagnostic facilities at MI Clinic are a cyclotron, three PET/CT systems, two MRI systems, and three ultrasound systems (all from GE), plus a FUJIFILM mammography system and a Shimadzu dedicated breast PET system. Approx. 7,000 PET/CT examinations are performed each year, of which 75 % are provided under health insurance and 501 are performed by the Shimadzu Elmammo dedicated breast PET (hereafter “dbPET”) system (of which 88 % or 441 are screenings). At present, MI Clinic has 10 radiological technologists (6 men and 4 women) and all breast examinations are performed by female technologists.

Fig.1 External View of MI Clinic

2. Introduction

Despite increasing rates of morbidity and mortality for breast cancer, Japan has a low mammogram screening rate compared to other countries. This disparity is believed to be due to patients’ aversion to pain caused by breast compression and dislike of one’s breasts being handled. Mammograms also have difficulty showing tumors in dense breast tissue that is commonly present in young women.

Meanwhile, dbPET examinations cause almost no pain and require almost no handling of the breasts. Examinations are performed in a prone position with each breast placed alternatively in a single detector hole. This position reduces movement due to respiration and, because the breast hangs perpendicular from the body, allows visualization of a larger area of the breast. The detector is also equipped with high-resolution depth of interaction (DOI) technology that determines the depth of detected tumors. The close proximity of the breast and detector in the dbPET system improves both examination sensitivity and spatial resolution and allows the detection of even small breast cancers **(Fig. 2)**. It has also been reported that lesions in high density breast tissue are clearly visualized by dbPET and utilizing dbPET in an ancillary role to mammographic screening could help in the detection of early breast cancers. In July 2013, dbPET was

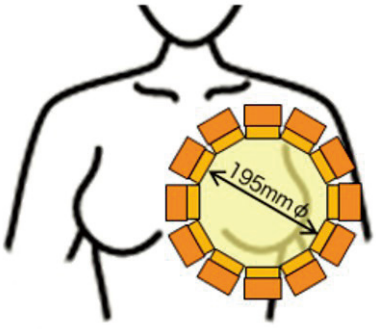

Fig.2 Detector Layout (Detector Diameter: 195 mm)

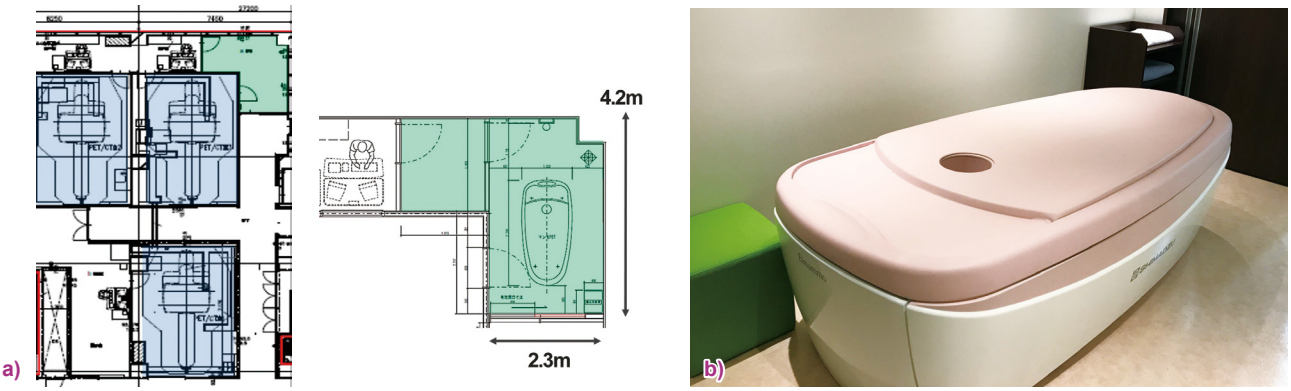

Fig.3 a) Refurbishment of Controlled Area (Changes only made to ■ area. Left: before changes, Right: after changes)
The compact design of the Shimadzu dbPET system allowed installation in a confined area of 2.3 m × 4.2 m.
b) dbPET room

listed for health insurance coverage when performed in combination with whole-body PET/CT, and in 2015, MI Clinic procured a Shimadzu dbPET system.

3. Course of Events up to Clinical Use

3.1 Process

dbPET systems are subject to regulations on the use of unsealed radiation sources, hence MI Clinic sent a notification of use to the Nuclear Regulation Authority, and in July 2015, submitted a written application for permission for partial change to a public health center. In August, work began on converting a storage room into a dbPET examination room and control room **(Fig. 3a)**. After consulting with female staff, the room interior was decorated to resemble the relaxing atmosphere of a salon with indirect lighting, tasteful curtains, and calming music **(Fig. 3b)**. The system was installed and phantom imaging and volunteer imaging were performed in September, and in October private practice and health insurance treatment began. In private practice cases, MI Clinic explains that the dbPET system is specifically for breast cancer screening and must be combined with other examinations, and performs examinations once the patient is satisfied.

3.2 Investigations

(1) Waiting Time

At MI Clinic, the normal waiting time from FDG administration to whole-body PET/CT is 60 minutes, and assuming the time needed for dbPET is 15 minutes and for whole-body PET/CT is 25 minutes, dbPET examinations were performed in a healthy volunteer 40, 90, and 120 minutes after FDG administration **(Fig. 4)**. Comparing these images showed a waiting time of 40 minutes resulted in inadequate FDG uptake with uneven uptake by normal mammary gland tissue. Based on this finding and also to reduce X-ray dose levels received by radiological technologists during examination tasks, a waiting time of 90 ± 5 minutes was selected.

(2) Scanning Time

Data was acquired for 10 minutes and images were reconstructed based on data acquired after scanning times between 3 and 10 minutes **(Fig. 5)**. Extending the imaging time reduced noise and

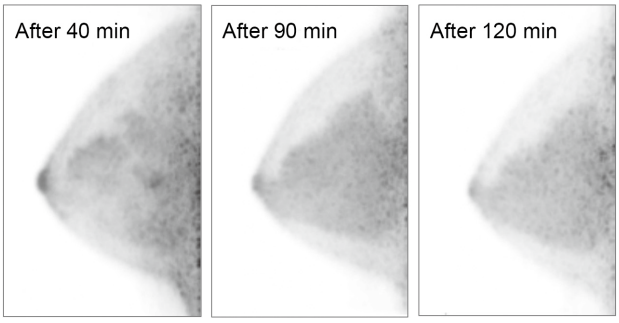

Fig.4 dbPET Images of a Healthy Volunteer

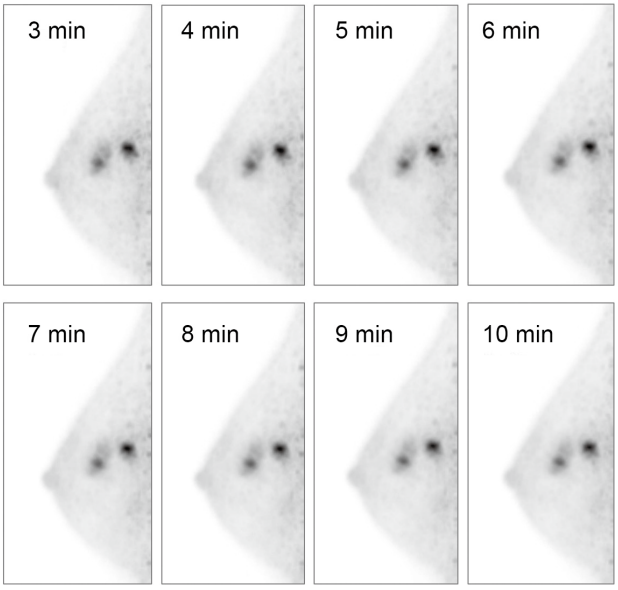

Fig.5 Comparing Images at Different Data Acquisition Times

improved image quality, but also the reconstruction time become longer for about the same amount and negatively affected throughput. Subjects also complained of discomfort after bending the neck for an extended period in the prone position, hence the normal imaging time was set to 5 minutes per side. For delayed phase imaging, a waiting time of 120 minutes and an scanning time of 7 minutes per breast were selected with an imaging start time of up to ± 5 minutes.

(3) Positioning

It is said that the patient positioning is simple because the dbPET system reconstructs two directions in real time then can be simply displayed on a monitor, but the blind area of chest wall is a weak point. In our clinic, a towel is placed in the lower abdomen of the breast on the examination side to minimize the blind area and to provide a wider view of the area with the most mammary glands **(Fig. 6a)**, and the radiologist gently presses against the shoulder blade to prevent a gap between the size of the image and the type of mammary gland. These measures help position the breast deeper in the detector hole **(Fig. 6b)**.

(4) Display and Outputs

Because dbPET systems produce high-resolution three-dimensional tomographic images, MI Clinic follows the 2019 clinical practice guideline for high-resolution breast PET that recommend, “concerning images similar to mammographic images, prepare ML and CC-MIP images, and prepare tomographic images in three directions (transverse, sagittal, and coronal images).” When saving images, images are first verified on a monitor at a fixed maximum standardized uptake value (SUV), after which density is adjusted based on background mammary glands. In patients with past examination history, past images are used as reference (SUV value) and, when saving images, images are prepared at the appropriate density for each patient.

4. Case Study

4.1 Case 1: 43 Years Old, Histology: Phyllodes Tumor (Fig. 7)

This case presented with dense breast tissue. A tumor that was not clearly identified by mammography but was revealed by dbPET as clear FDG uptake (SUVmax: 5.5) in the upper inner/upper outer quadrants of the right breast. In this case, the tumor was found only because dbPET produces high-contrast images that are less affected by background mammary glands.

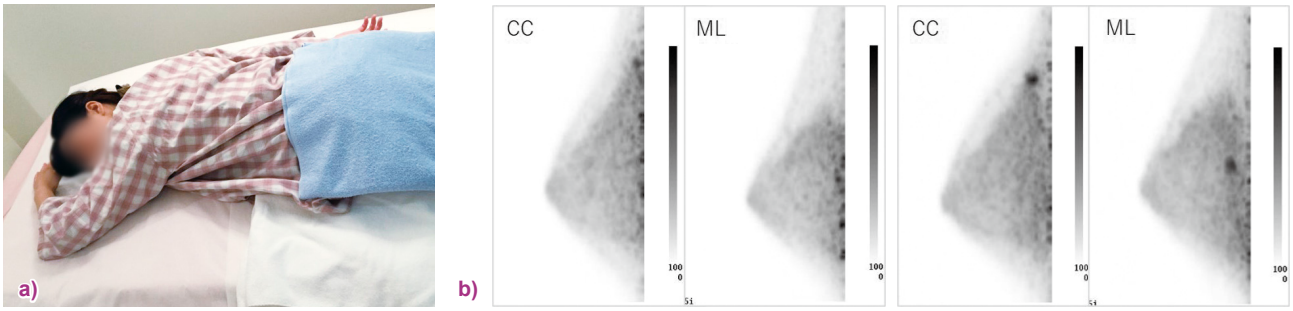

Fig.6 **a)** Towel Placed on Unexamined Side during Positioning
b) Images that Show the Importance of Positioning. Left: Poor Positioning, Right: Amended Positioning

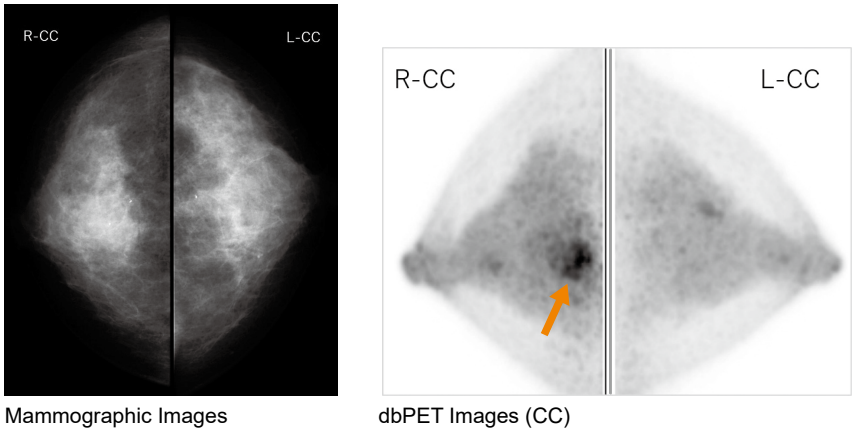

Mammographic Images dbPET Images (CC)

Fig.7 Tumor Discovered in Patient with Dense Breast

4.2 Case 2: 77 Years Old, Histology: Mucinous Carcinoma (Fig. 8)

Whole-body PET/CT and dbPET were performed after contrast-enhanced breast MRI revealed a 25-mm tumor (➡) near the upper inner/upper outer quadrants and central portion of the left breast and a 10-mm daughter nodule (➡) on the boundary between the upper inner and upper outer quadrants. Examination of the 25-mm tumor (➡) by whole-body PET/CT revealed strong FDG uptake throughout the entire mass while contrast-enhanced MRI and dbPET revealed the tumor was ring-shaped. The daughter nodule (➡) was also found in the same position by MRI and dbPET, which indicates the diagnostic performance of dbPET is equivalent to that of contrast-enhanced MRI. Accordingly, dbPET is an effective substitute when MRI is contraindicated due to an allergy to contrast medium or implanted metal.

4.3 Case 3: 47 Years Old, Histology: Intraductal Papilloma (Fig. 9)

dbPET revealed abnormal uptake (SUVmax: 4.5) in the upper outer quadrant of the right breast and biopsy revealed intraductal papilloma. As shown in this case, because FDG can also be metabolized by benign tumors, it is important to make a conprehensive judgment with other modalities.

4.4 Case 4: 71 Years Old, Histology: Invasive Ductal Carcinoma (Fig. 10)

Breast ultrasonography revealed a 17-mm diameter hypoechoic region in the upper outer quadrant of the right breast that was diagnosed as invasive ductal carcinoma (triple negative type) after core needle biopsy and was subject to further preoperative examinations. Whole-body PET/CT revealed a non-significant level of FDG uptake (SUVmax: 1.5), but dbPET revealed FDG uptake (SUVmax: 3.4→2.4) in the upper outer quadrant of the right breast. Since FDG uptake sometimes does not increase during delayed phase imaging of breast cancer, this difference in FDG uptake was attributed to histology in this case, and further investigations such as subtyping are considered necessary.

4.5 Case 5: 54 Years Old, Histology: Invasive Ductal Carcinoma (Fig. 11)

After 6 months of neo-adjuvant chemotherapy for left breast cancer (cT2N1M0, luminal B), whole-body PET/CT and dbPET were performed to determine the response. Whole-body PET/CT had revealed

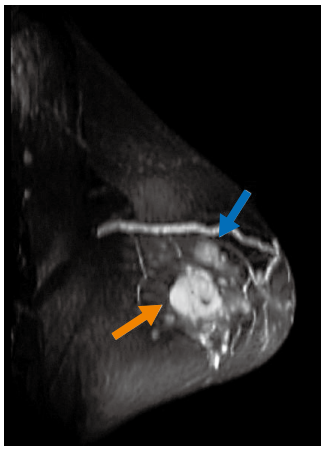

Contrast-Enhanced MRI Image (MIP)

T1 Sag FS Image

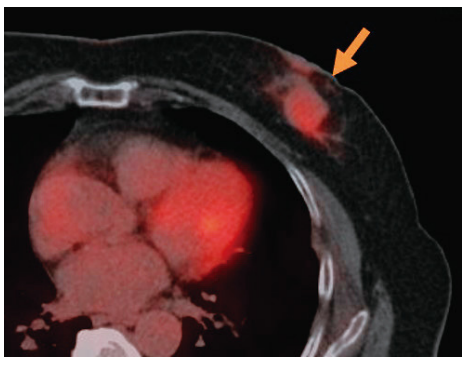

Whole-Body PET/CT Image (Axi)

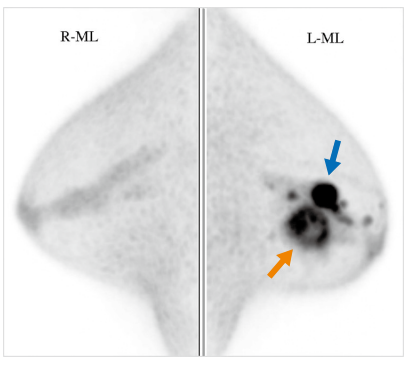

dbPET Images (ML)

Fig.8 dbPET Helpful in Diagnosis of Cancer Extent

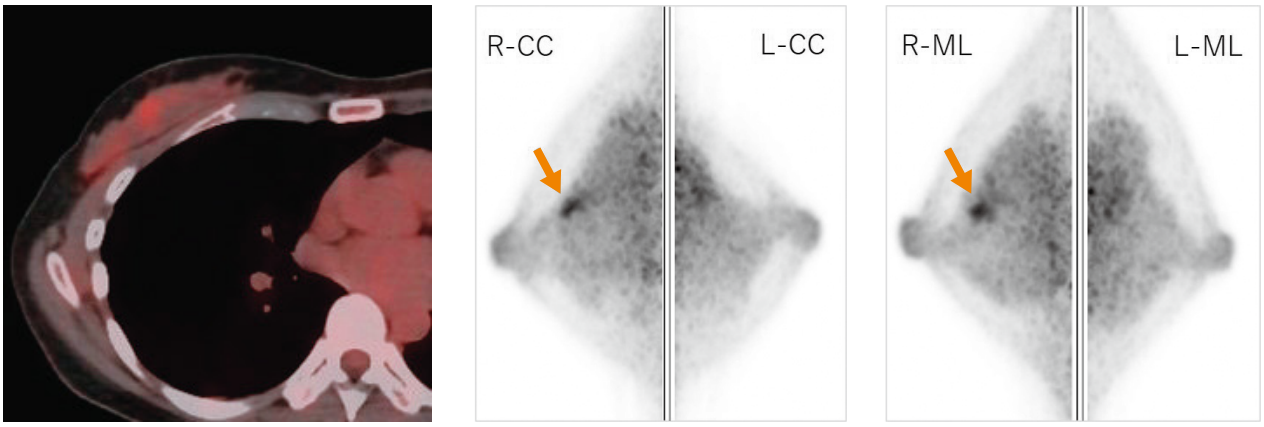

Whole-Body PET/CT Image (Axi) dbPET Images (CC) dbPET Images (ML)

Fig.9 False-Positive Case

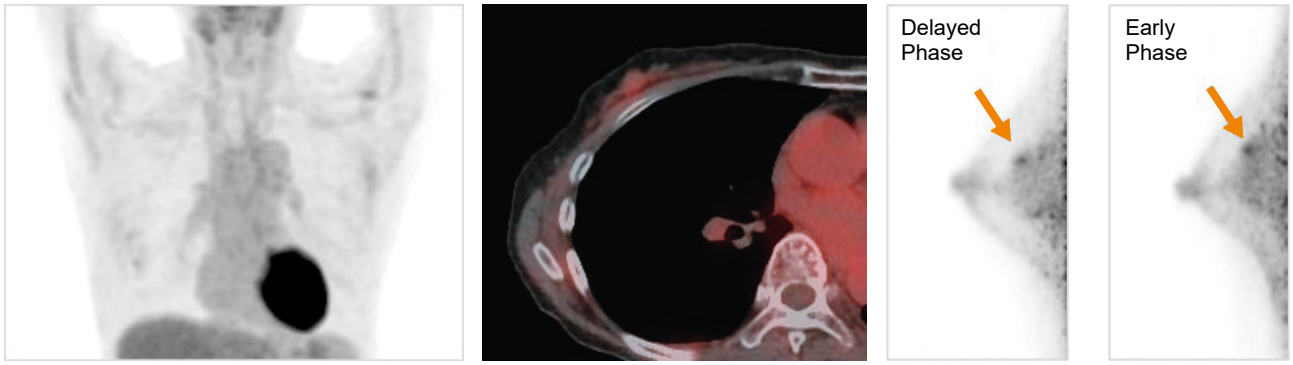

Whole-Body PET MIP Image Whole-Body PET/CT Image (Axi) dbPET Images of Right Breast (CC)

Fig.10 False Negative Case (Breast Cancer with Reduced FDG Uptake in Late Phase)

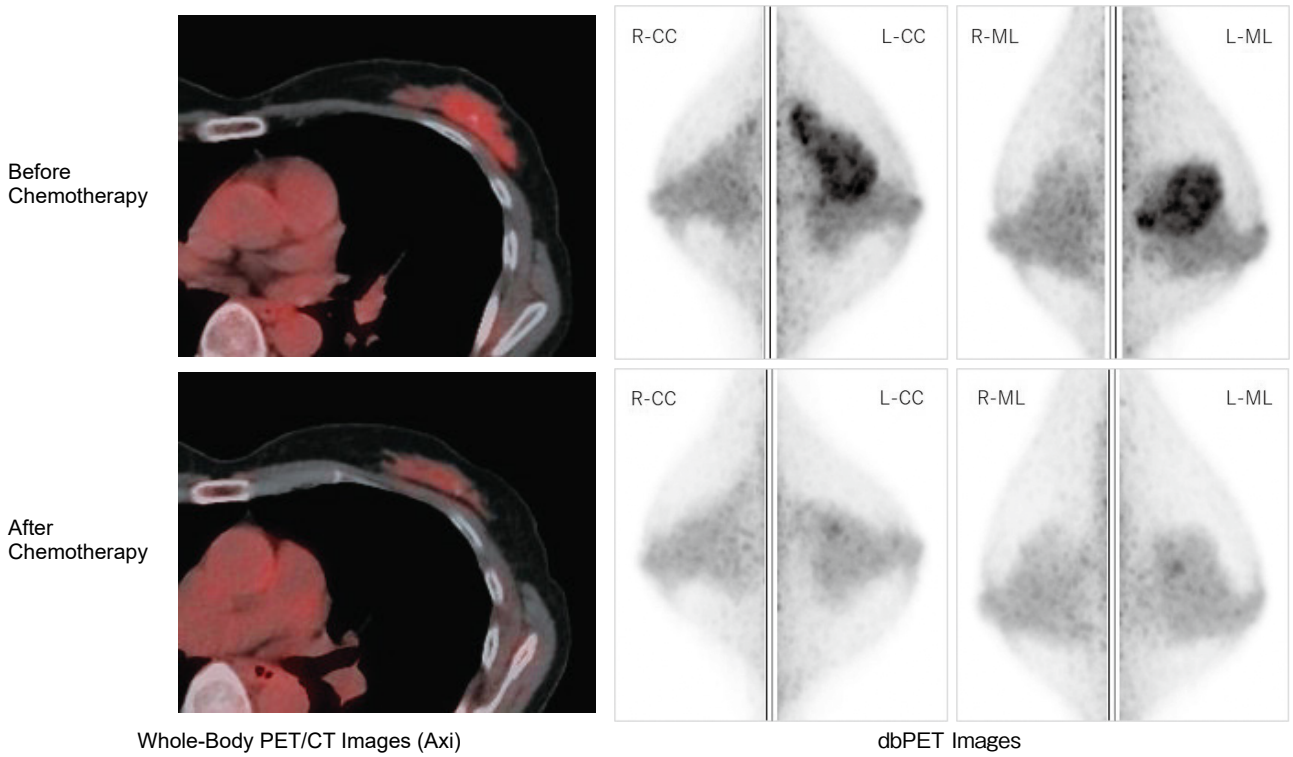

Whole-Body PET/CT Images (Axi) dbPET Images

Fig.11 Before and after Neo-Adjuvant Chemotherapy

FDG uptake (SUVmax: 3.1) in the upper outer quadrant of the left breast but images acquired after chemotherapy showed no FDG uptake and a complete response (CR) was determined based on diagnostic imaging. By contrast, dbPET revealed FDG uptake (SUVmax: 2.1) in the upper outer quadrant of the left breast even after chemotherapy, and residual tumor activity was deemed a possibility based on diagnostic imaging. This case was identified thanks to the superior sensitivity and spatial resolution of dbPET compared to whole-body PET/CT.

4.6 Case 6: 47 Years Old, Histology: Invasive Ductal Carcinoma (Fig. 12)

Examinations were performed to search for distant metastasis before administering neo-adjuvant chemotherapy for stage IIIb left breast cancer (T4bN1M0). Whole-body PET/CT and dbPET both revealed nodular FDG uptake (➡) in the left breast, but only dbPET revealed punctiform FDG uptake in the upper outer quadrant of the right breast. Further investigation of the right breast revealed stage 0 breast cancer (TisN0M0). This case shows that dbPET can identify unexpected lesions and have a major effect on treatment strategy.

4.7 Case 7: 42 Years Old, Histology: Flat Epithelial Atypia (FEA) (Fig. 13)

Screening was performed by breast ultrasonography, whole-body PET/CT, and dbPET. Ultrasonography and whole-body PET/CT failed to identify any anomalies, but dbPET revealed FDG uptake (SUVmax: 5.7) in the central portion of the right

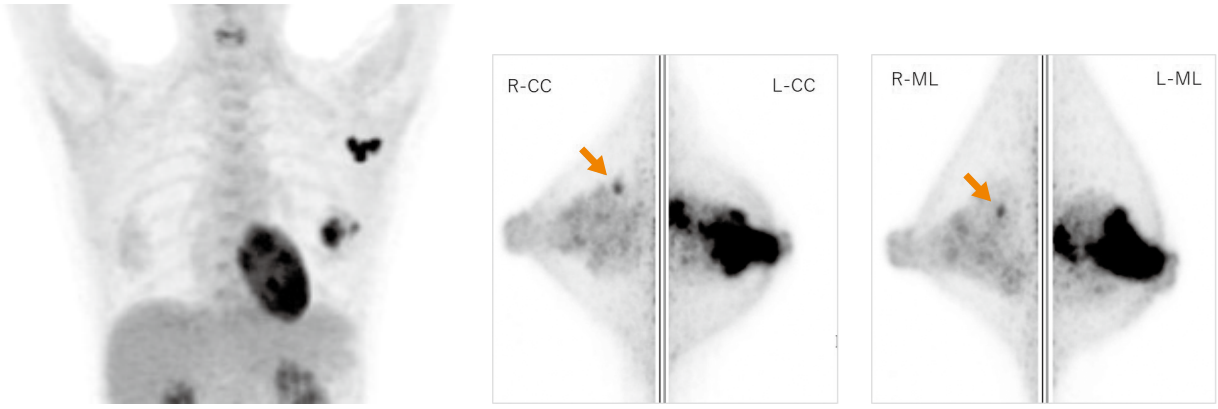

Whole-Body PET MIP Image　　dbPET Images

Fig.12 Accidental Discovery of Contralateral Breast Cancer

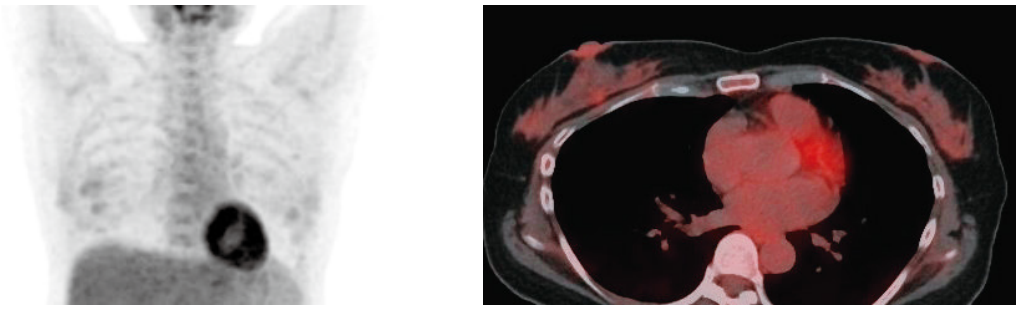

Whole-Body PET MIP Image　　Whole-Body PET/CT Image (Axi)

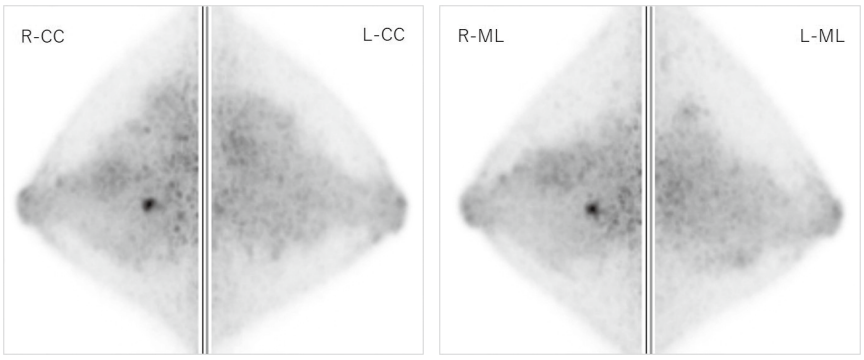

dbPET Images

Fig.13 Lesion Detected at Very Early Stage

breast. In these situations, the finding is reported to the technologist responsible for ultrasonography and another ultrasound (second-look ultrasonography) is performed if required. In this case, even second-look ultrasonography failed to identify the tumor. Contrast-enhanced ultrasonography performed by a referral institution revealed a 5-mm tumor in the central portion of the right breast and biopsy revealed FEA (the earliest histological sign or a precursor lesion of low grade DCIS). In this case, dbPET was deemed exceptional as the only modality that discovered the tumor at a very early stage.

5. Conclusion

Since MI Clinic procured a dbPET system and commenced screening for all types of breast cancer, the number of women examined in 2019 has doubled compared to 2014 before procurement, and the rate of repeat clients is 40 %. This increase is thanks to a dbPET system that accommodates patient wishes for painless breast cancer screening. Using dbPET in combination with whole-body PET/CT also offers the advantage of revealing unexpected diseases outside the breasts. The diagnostic performance of dbPET is similar to that of contrast-enhanced MRI, and given that MRI has been listed for health insurance coverage in April 2020 in cases of hereditary breast and ovarian cancer (HBOC) syndrome, clinical research is expected to commence into using dbPET for the same condition. If dbPET is shown to be effective for HBOC, it promises to play an increasingly useful role in the growth of breast cancer screening. MI Clinic is also committed to working with other facilities towards this goal.

Editor's note:

The availability of this product is regionally limited due to regulatory or other reasons. Please contact Shimadzu's local representative to confirm it in your country.

PET

TOF-PET System Development of BresTome™

Medical Systems Division, Shimadzu Corporation
Atsushi Ohtani

1. Introduction

Positron emission tomography (PET) emerged from the field of research into brain function. FDG was also a PET drug developed to target the brain that visualizes glucose metabolism. Later, FDG was also recognized to be useful for cancer screening, which led to the increased prevalence of whole-body PET systems for use in cancer screening and the continued development of whole-body PET systems to this day. Recently, whole-body PET image resolution has been approaching a theoretical limit due to the size of the ring diameter (clear bore) used by PET scanners that image the whole body.

Since it launched the first dedicated head PET/SPECT system in 1981, Shimadzu has released many PET systems to market. To achieve image resolutions unattainable by scanners with large bore diameters, Shimadzu has developed the BresTome TOF-PET system that produces high-resolution PET images of the head and breast by positioning new high-resolution PET detectors with inbuilt time of flight (TOF) function proximally to the subject. The name BresTome is an abbreviation of “Brain and Breast Tomography for rest,” intended to represent a head and breast tomography system designed for comfort. This article describes the BresTome dedicated the head and breast TOF-PET system that was approved by the Japan’s Pharmaceuticals and Medical Devices Agency in October 2020.

2. System Features

2.1 Compact Design

BresTome has a compact design comprised of two parts: the main system unit that integrates the PET scanner, bed, and console equipped with a screen for GUI and panels to move the PET scanner; and a terminal (operating box) used to start imaging from an operation room. A remote terminal (subterminal) that can operate the screen on the main system unit from an operation room is also available as an optional product **(Fig. 1)**.

2.2 Simple Subject Positioning

When imaging the head, the subject lies supine with their head placed on a headrest, and when imaging the breast, the subject lies prone with a breast suspended in the detector hole. The operator moves the PET scanner to the examined site via the scanner control panel in the console **(Fig. 2)** and checks positioning via a real-time viewer that displays planar images in two views. Because the real-time viewer is displayed on a monitor in the console integrated into the main system unit, the operator can quickly complete positioning while checking both the position of the subject and the real-time viewer without moving between the examination room and operation room.

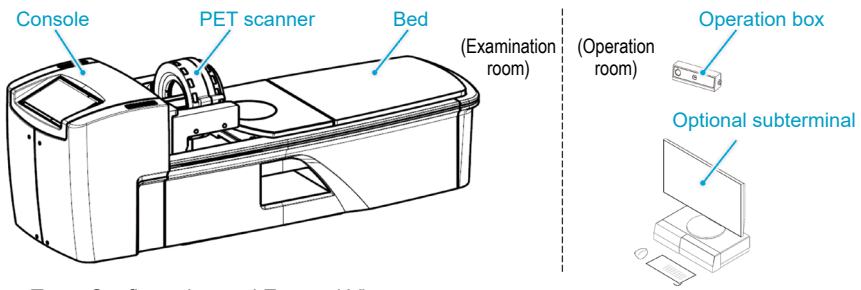

Fig.1 BresTome Configuration and External View

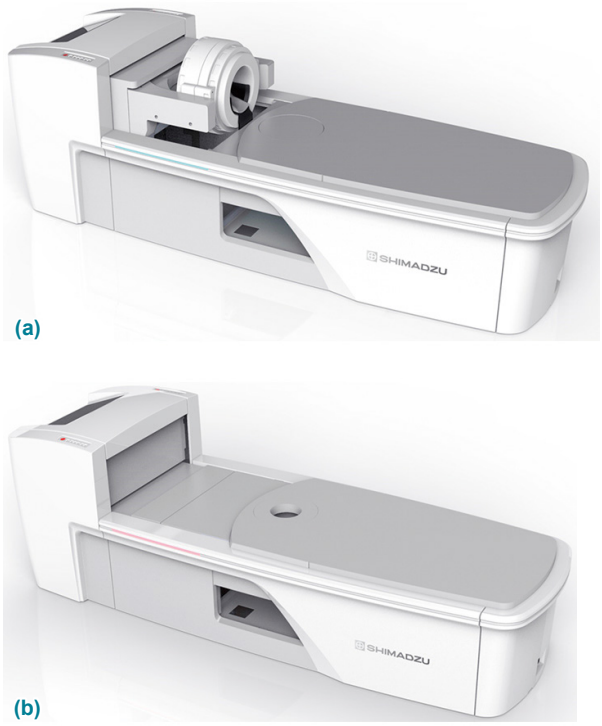

Fig.2 PET Scanner Movement Complete (for Head Imaging (a) and for Breast Imaging (b))

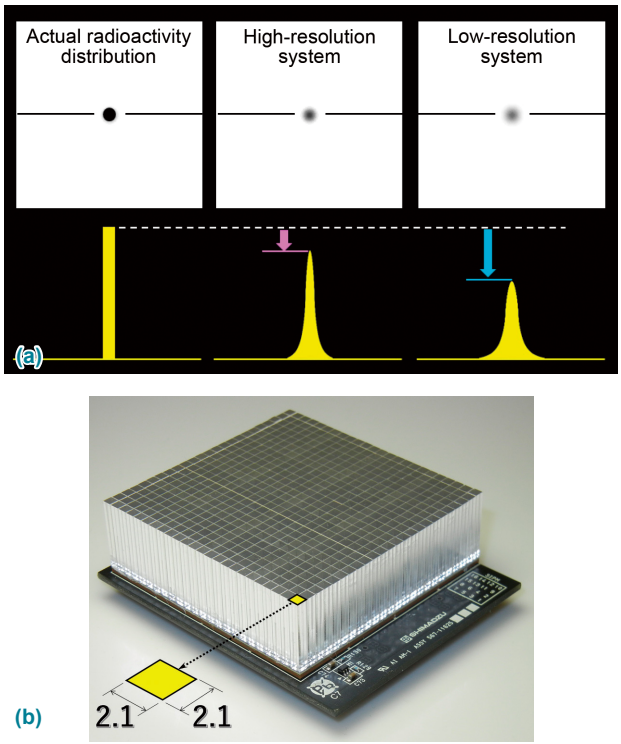

Fig.3 Schematic Diagram of Partial Volume Effect (a) and BresTome TOF-PET Detector (b)

2.3 High-Resolution Detector

The physical characteristics of PET systems cause a partial volume effect that lowers an object's radioactivity distribution at each pixel and reducing visualization performance (Fig. 3a). This shortcoming has created a need for technical innovations that increase image resolution and reduce the partial volume effect. In one usage case, when diagnosing metastatic spread to small lymph nodes during cancer staging, such higher resolution images should help lower the likelihood of false negatives. High-resolution PET images require a small-form PET detector that has been optimized by combining very small scintillators with highly sensitive optical light-receiving elements with many light-receiving elements. Shimadzu achieved high-resolution PET imaging by combining new technology with PET detector technology cultivated by Shimadzu over the course of more than 40 years, and developed a small-form TOF-PET detector (Fig. 3b) capable of rapidly processing signals from scintillators that contain lutetium and silicon photomultipliers (SiPMs). In TOF-PET systems, the higher the TOF resolution performance, the better the PET image S/N ratio (TOF-Gain). BresTome achieves approx. 4 times the TOF-Gain when examining heads and other objects that are approx. 20 cm in diameter, promising images with an equivalent S/N ratio in just 1/4 the imaging time and without conventional TOF information.

2.4 Effective Field of View Optimized for Head and Breast Imaging

One more technique used to achieve high-resolution imaging is to arrange 16 small-form TOF-PET detectors in a ring in close proximity to the subject. A bore diameter of 283 mm is large enough to image the head, and also allows insertion of the breast up to the chest wall within the scan field of view during breast imaging. Arranging a maximum of three detectors axially also provides a 162 mm axial field of view (AFOV) capable of imaging the entire brain in a single acquisition (static). Stepwise movement of the PET scanner in the axial direction also provides a maximum AFOV of 200 mm capable of imaging even large breasts (Fig. 4).

2.5 Attenuation Correction without Additional Exposure

BresTome is equipped with a boundary method[1)] that corrects for uniform absorbers based on emission data from PET drugs and a TOF-based maximum-likelihood attenuation corrector factor (ML-ACF) method[2)] that corrects for non-uniform absorbers using TOF information. These methods prevent additional exposure via external radiation from either CT or external radiation sources used for attenuation correction.

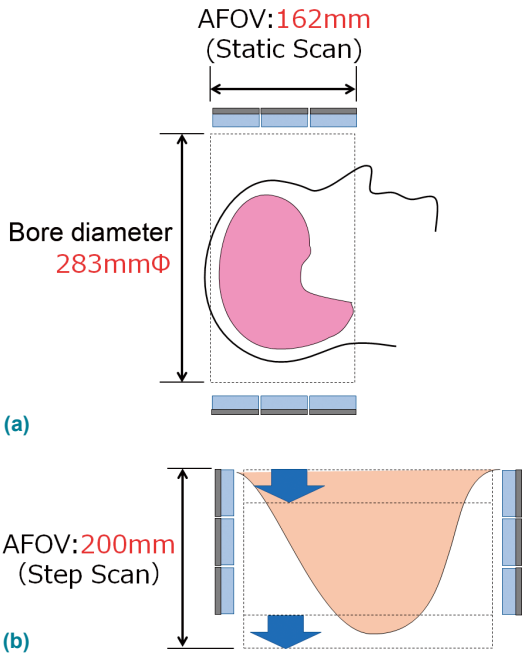

Fig.4 AFOV during Static Acquisition (a) and Step-and-Shoot Acquisition (b)

3. Applications

BresTome produces diagnostic images in the form of detailed information on the distribution of positron radioactive drugs in the head and breast after administration of a positron radioactive drug. For breast imaging, patients examined in a whole-body PET system can undergo a breast PET examination with BresTome on the same day without the administration of additional PET drugs. For head imaging, head PET examinations for epilepsy and brain function are performed using only BresTome (when there is no obvious medical need to use a whole-body PET system and BresTome on the same day), but in other situations, head PET examinations with BresTome are performed on the same day the subject is examined with a whole-body PET system (Fig. 5). Fig. 6 and 7 show images obtained with a prototype BresTome system and MRI/FDG-PET fusion images.

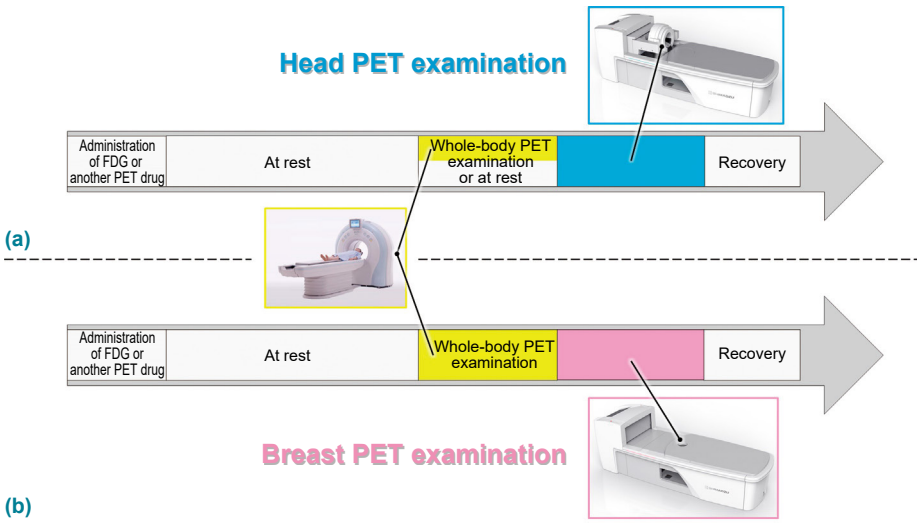

Fig.5 Example Examination Flow: Head PET Examination (a), Breast PET Examination (b)

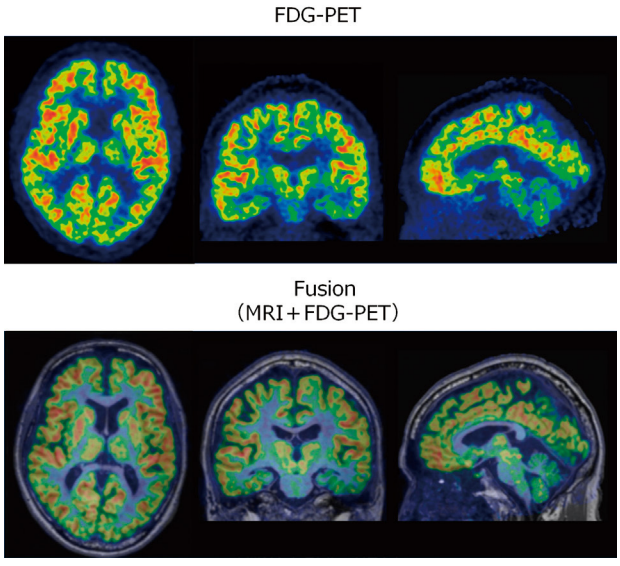

Fig.6 Head FDG-PET (Slice) Images (Top) Obtained with Prototype System and MRI/FDG-PET Fusion (Slice) Images (Bottom)

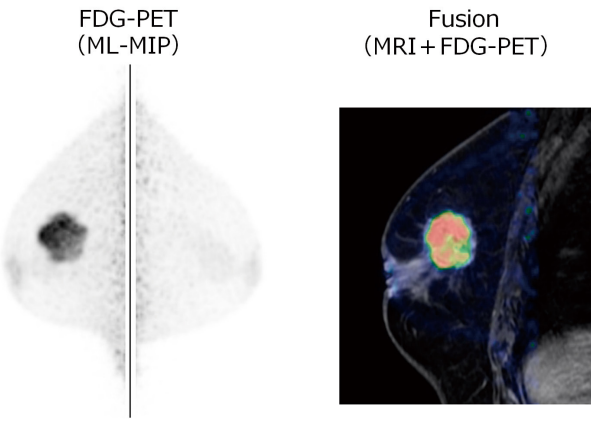

Fig.7 Breast FDG-PET (ML-MIP) Images (Left) Obtained with Prototype System and MRI/FDG-PET Fusion (Slice) Images (Right)

4. Conclusion

In recent years, PET drugs approved for use in Japan or overseas have allowed the visualization of amyloid beta peptides in Alzheimer's dementia, dopamine transporters in Parkinson's disease, and estrogen receptors in breast cancer. There are also growing hopes for the establishment of diagnostic methods that use PET drugs to visualize methionine in brain tumors and tau proteins in dementia. Immune checkpoint inhibitors and photoimmunotherapy are also emerging as new treatments for breast, head and neck, and other cancers, and there are hopes that PET examinations may be selected to determine the therapeutic effect of these new treatments[3]. Such diagnostic investigations require visualization, staging, and elucidation of localized lesion sites that, it is believed, will increase the demand for BresTome, a PET system designed to examine specific sites with excellent resolution.

BresTome is expected to play a role in new medical care and research beyond the role played by PET in medical care to date. Going forward, Shimadzu intends to investigate the utility of PET examinations with BresTome and establish examination methods for BresTome while also pursuing other technical innovations.

Lastly, Shimadzu is extremely grateful to Professor Kazunari Ishii of the Department of Radiology, Faculty of Medicine, Kindai University who plays the role of principal investigator in clinical research using the prototype BresTome system, and to the physicians and faculty of Kindai University Hospital and the Division of PET Molecular Imaging, Institute of Advanced Clinical Medicine, Kindai University. Shimadzu is grateful to the many parties who provided considerable assistance and advice in the development of BresTome.

References

1) Liang-Kai Huang, etc. : Image thresholding by minimizing the measures of fussiness, Pattern Recognition, Vol. 28, No.1 pp41-51, 1995
2) Michel Defrise, etc. : Time-of-flight PET data determine the attenuation sinogram up to a constant, Phys. Med. Biol., 57, 885-899, 2012
3) Shinsuke Sasada, etc. : Dedicated breast PET for detecting residual disease after neoadjuvant chemotherapy in operable breast cancer: A prospective cohort study. EJSO Vol.44, Issue 4:444–448, 2018

Editor's note:

This product is not available outside of Japan as of Feb. 2021. Please contact Shimadzu's local representative to confirm its latest availability for your country.

Stories of Kyoto-born Masterpieces — 24

Numerous outstanding products have helped shape the history of Kyoto — here we outline the stories hidden behind them.

From above, *tsuzura* to hold stationery, obi belts, and kimono. All the *tsuzura* are made to order, and customers can choose the type of coating and whether to have their family crest on the side. *Akeni* boxes for the sumo world, such as that shown to the far left, are all made at Watanabe Shoten.

Kyo-tsuzura — Storage Baskets

Beautifully weaved bamboo and closely wrapped *washi* paper. Coatings of persimmon tannin and cashew lacquer, and a family crest on the side to complete the item's grand appearance. Simply put, *tsuzura* are lidded storage baskets made of bamboo. Fans of historical dramas might have seen them being piled onto two-wheeled carts as the characters escape from fire.

Tsuzura originated in China, and early models weaved from rattan and willow have been preserved at the Shoso-in Repository in Nara. The basket's materials evolved with the times, and in the Edo period, they came to be weaved from thinly cut pieces of bamboo and Japanese cypress.

Tsuzura have long been valued for their excellent breathability, as well as their insect-repellant, preservative, and dampproof properties, and the persimmon tannin plays a key role in these functions. Due to these qualities, *tsuzura* have been used since long ago to store kimono and obi belts at kimono stores, kabuki costumes, hanging scrolls used at tea ceremonies, museum artwork, and more. *Tsuzura* are also used as *akeni* boxes, which are presented to sumo wrestlers when they reach juryo ranking. Other than the fact that the edges are reinforced with metal—as the boxes are frequently pulled along tatami mats and used as stools—*akeni* are the same as *tsuzura*. Both *akeni* and *tsuzura* must be robust, and this is exactly why they are made of hard moso bamboo.

Wet, Dry, and Repeat

The moso bamboo used in *Kyo-tsuzura* is taken from bamboo thickets between the Rakusai and Nagaokakyo areas of Kyoto. They are cut down after two to three years of growth, and taken to the workshop while still green. The bamboo is roughly cut vertically before being cut into finer sheets. In the next step, the sheets of bamboo are sliced into thin strips using a special blade known as a *hegi-bocho*. Using only feel, cutting the strips into even thicknesses is an extremely difficult task that can only be undertaken by expert craftsmen.

Despite being from the same thicket, each piece of bamboo has different properties and varying levels of hardness. As such, the thickness of each strip depends entirely on the bamboo's hardness, and is determined based on the flexibility of each piece. Each strip is then seared with a burner for a few seconds before being bent into a U-shape, and then instantly cooled in water. After repeating this process with the necessary quantity of strips, the next step is to weave them together.

The weaving pattern is known as *yotsume-ami*, with alternating horizontal and vertical pieces of bamboo. While moistening the bamboo with a water from a spray bottle, the craftsman weaves the strips into a grid pattern with equal spaces between each. The bamboo is left to dry once the weaving is complete. Generally,

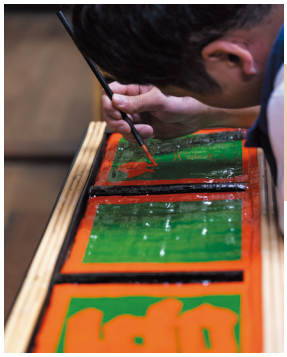

The fourth generation of the Watanabe family is in charge of lettering. *Akeni* boxes stand out for their vermillion characters.

Slicing the bamboo into strips under 1 mm thick is the most difficult part of the process, one which is said to take up to ten years to learn.

Coating a *washi*-covered basket (left) with persimmon tannin (right), adds to the basket's character. For *tsuzura* that hold museum artworks, cashew lacquer is rarely applied, with many simply coated in persimmon tannin as above.

The bamboo is vigorously cut into rough sections before being cut again into sheets.

The two knives in the middle are *hegi-bocho*, while the two tools on the right are for applying the *washi*. The *kaki-take*, which resembles a Japanese tea whisk, is handmade and helps to ensure the glue reaches every corner.

The bamboo strips are seared with a burner and bent into a U-shape. These strips are then used to create the *yotsume-ami* pattern.

each step in the process involves repeated wetting and drying, and the bamboo must be completely dry before the craftsman can move onto the next step.

Next, starch glue—into which persimmon tannin has been mixed—is applied to the dry bamboo using a brush made by hand from the ears of a rice plant. *Washi* paper is affixed to both the inside and the outside of the basket, and it is the gaps between the *yotsume* pattern that help to ensure the *washi* is firmly attached to the basket. As the fibers of the *washi* combine well with the glue, the *washi* provides structural support to the bamboo and ensures a robust finish. After the *washi* paper has been affixed to the inside of the basket, mosquito net material—which has been backed with *washi* paper itself—is applied to the frame of the basket to reinforce the structure, before *washi* is applied to the outside. To finish, the outside is coated with persimmon tannin (and cashew lacquer if desired) and decorative paper is stuck on the inside. Each process takes up to a day, and with 25 different stages involved, the creation of a single *Kyo-tsuzura* requires more than a month.

A Natural Storage Basket to Carry on into the Future

Previously, the creation of *tsuzura* baskets was undertaken at separate workshops, with one responsible for the bamboo basket, and another taking charge of the *washi* and coating. As the popularity of Western-style clothes and wardrobes increased, however, general demand for *tsuzura* baskets plummeted. Many craftsmen were driven out of the business, and ultimately, only the Watanabe family in Kyoto remained. The father of Yoshikazu Watanabe—third-generation and current head of Watanabe Shoten—who was previously in charge solely of creating the bamboo baskets, set out to undertake the entire process including the *washi* and coating. It is thanks to him that we still have *Kyo-tsuzura* today. "If the air is moist, the fibers of the bamboo absorb water and expand. When the air dries, the fibers slowly release the water. In effect, the bamboo is breathing. This is why *tsuzura* prevent damage to kimono embroidery and keep all the threads intact," says Yoshikazu Watanabe. Not only is it the persimmon tannin that contributes to the functionality of *tsuzura* baskets, but the innate properties of the bamboo, too.

Kyo-tsuzura combine beauty, functionality, and sustainability. Stains and scratches only serve to give the *tsuzura* character, and applying new *washi* layers gives the basket a new life. *Kyo-tsuzura* are masterpieces that can hold valuable items and stay with the owner long into the future.

Special thanks to: Watanabe Shoten; +81-75-551-0044

MEDICAL NOW Digest

www.shimadzu.com/med

6032-11003-1TD
ISSN0916-8745